

This paper is published as part of a *Dalton Transactions* themed issue entitled:

Application of inorganic chemistry for non-cancer therapeutics

Guest Editor: Katherine J. Franz

Published in issue 21, 2012 of *Dalton Transactions*

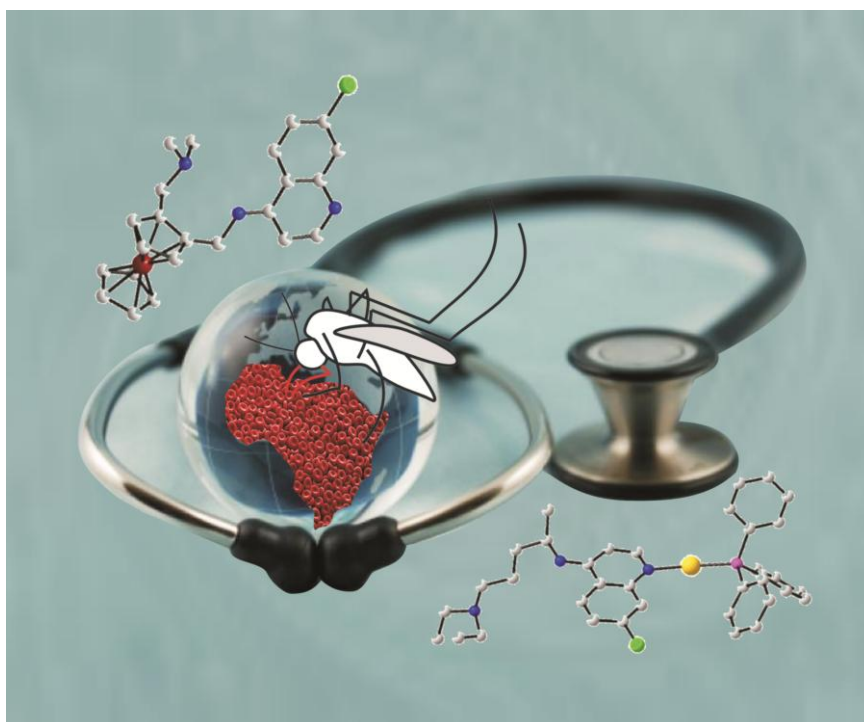


Image reproduced with permission of Christophe Biot

Articles published in this issue include:

[The therapeutic potential of metal-based antimalarial agents: Implications for the mechanism of action](#)

Christophe Biot, William Castro, Cyrille Y. Botté and Maribel Navarro
Dalton Trans., 2012, DOI: 10.1039/C2DT12247B

[Chelation therapy in Wilson's disease: from D-penicillamine to the design of selective bioinspired intracellular Cu\(I\) chelators](#)

Pascale Delangle and Elisabeth Mintz
Dalton Trans., 2012, DOI: 10.1039/C2DT12188C

[Therapeutic potential of selenium and tellurium compounds: Opportunities yet unrealised](#)

Edward R. T. Tiekink
Dalton Trans., 2012, DOI: 10.1039/C2DT12225A

Visit the *Dalton Transactions* website for more cutting-edge bioinorganic chemistry research

www.rsc.org/dalton

Cite this: *Dalton Trans.*, 2012, **41**, 6536

www.rsc.org/dalton

PAPER

Heterocyclic dithiocarbazate iron chelators: Fe coordination chemistry and biological activity†

Maram T. Basha,^a Jy D. Chartres,^a Namfon Pantarat,^b Mohammad Akbar Ali,^c Aminul Huq Mirza,^c Danuta S. Kalinowski,^b Des R. Richardson^{*b} and Paul V. Bernhardt^{*a}

Received 11th December 2011, Accepted 13th January 2012

DOI: 10.1039/c2dt12387h

The iron coordination and biological chemistry of a series of heterocyclic dithiocarbazate Schiff base ligands is reported with regard to their activity as Fe chelators for the treatment of Fe overload and also cancer. The ligands are analogous to tridentate heterocyclic hydrazone and thiosemicarbazone chelators we have studied previously which bear *NNO* and *NNS* donor sets. The dithiocarbazate Schiff base ligands in this work also are *NNS* chelators and form stable low spin ferric and ferrous complexes and both have been isolated. In addition an unusual hydroxylated ligand derivative has been identified *via* an Fe-induced oxidation reaction. X-ray crystallographic and spectroscopic characterisation of these complexes has been carried out and also the electrochemical properties have been investigated. All Fe complexes exhibit totally reversible Fe^{III/II} couples in mixed aqueous solvents at potentials higher than found in analogous thiosemicarbazone Fe complexes. The ability of the dithiocarbazate Schiff base ligands to mobilise Fe from cells and also to prevent Fe uptake from transferrin was examined and all ligands were effective in chelating intracellular Fe relative to known controls such as the clinically important Fe chelator desferrioxamine. The Schiff base ligands derived from 2-pyridinecarbaldehyde were non-toxic to SK-N-MC neuroepithelioma (cancer) cells but those derived from the ketones 2-acetylpyridine and di-2-pyridyl ketone exhibited significant antiproliferative activity.

Introduction

In the treatment of acute iron (Fe) overload disorders, the administration of Fe chelating ligands is essential.^{1,2} In humans, intestinal Fe absorption is tightly regulated³ and when Fe levels are adequate, further Fe uptake is inhibited. In cases where severe Fe overload occurs, commonly through necessary blood transfusions in the treatment of anaemias such as β -thalassaemia, Fe overload becomes acute, as humans have no mechanism for actively excreting excess Fe. Failure to remove excess Fe leads to its accumulation in vital organs such as the heart and liver, and if left untreated, leads to irreversible organ damage and death.

Few Fe chelators have been successful in treating Fe overload in the clinic. Desferrioxamine (DFO; Chart 1) was for many years the only drug approved worldwide for the treatment of Fe overload. Its widespread use continues today, despite its major drawback of not being orally active.⁴ In fact, DFO must be

administered by long and frequent periods of subcutaneous infusion (12–24 h per day, 5–6 times a week). In 2005, the triazole deferasirox (Exjade®, Chart 1),^{5–8} was approved by the US Food and Drug Administration (FDA) for oral administration in the treatment of Fe overload and was the first drug of its type to be approved worldwide. However, possible side effects such as renal and liver damage and gastrointestinal haemorrhage in some patients were added as warnings to the packaging of this drug in 2010.‡

The hydroxypyridinones (such as deferiprone also known as L1 and more recently Ferriprox®) emerged in the 1980s⁹ and also offered the hope of oral activity, but controversy surrounding their efficacy and toxicity^{10,11} hampered drug development over the years. In 2011, the FDA finally granted approval for the ‘second line’ use of deferiprone as an orally administered drug in the treatment of Fe overload,§ although there are still unresolved questions over its efficacy. Notably, the most promising clinical results with deferiprone have been obtained when it is co-administered with DFO where it appears to be effective against Fe loading in heart tissue.¹²

The tridentate 2-pyridinecarbaldehyde isonicotinoyl hydrazone (HPCIH) family of Fe chelators (Chart 1) have shown

^aSchool of Chemistry and Molecular Biosciences, University of Queensland, Brisbane 4072, Australia. E-mail: p.bernhardt@uq.edu.au

^bDiscipline of Pathology, Sydney Medical School, University of Sydney, Sydney 2006, Australia. E-mail: d.richardson@med.usyd.edu.au

^cFaculty of Science, Universiti Brunei Darussalam, Gadong BE1410, Brunei Darussalam

† Electronic supplementary information (ESI) available. CCDC reference numbers 858720–858723. For ESI and crystallographic data in CIF or other electronic format see DOI: 10.1039/c2dt12387h

‡ <http://www.fda.gov/safety/medwatch/safetyinformation/safetyalertsforhumanmedicalproducts/ucm200850.htm>

§ <http://www.fda.gov/downloads/Drugs/InformationOnDrugs/UCM086233.pdf>

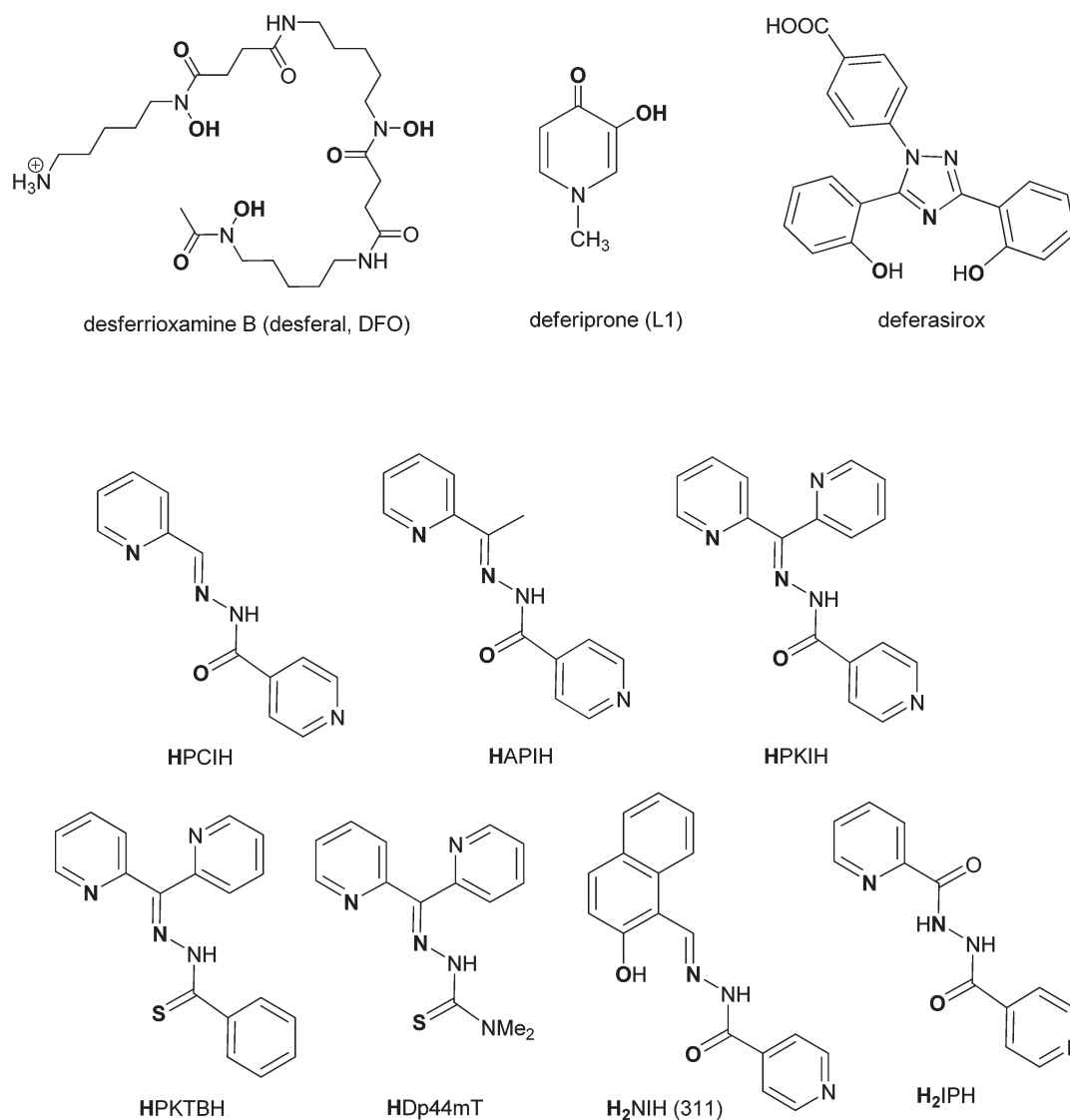


Chart 1 Fe chelators in clinical use for the treatment of Fe overload disease (*i.e.* DFO, deferiprone and deferasirox) as well as hydrazone, thiohydrazone, thiosemicarbazone and hydrazine Fe chelators with known biological activity. Donor atoms are in bold type.

promise as alternatives to existing compounds for the treatment of Fe overload.^{13–16} Investigations by our laboratories have shown that they form stable Fe^{II} complexes, in contrast to the Fe^{III} complexes formed by DFO, deferiprone and deferasirox.^{1,2,4} Subsequent studies have shown that substitutions to the C-atom adjacent to the pyridyl ring lead to a marked change in biological activity, for example the **HPCIH** analogues based on 2-acetylpyridine (**HAPIH** series)¹⁷ or di-2-pyridyl ketone (**HPKIH** analogues)¹⁸ exhibit significant cytotoxicity in contrast to the benign **HPCIH** chelators.¹⁶ Although deleterious for the treatment of chronic Fe overload (where chelators must be administered lifelong), cytotoxic Fe chelators may prove to be a novel and effective method in cancer therapy.^{19–26} Of interest, a significant increase in cytotoxicity and activity against neoplastic cells was found by substitution of the *O*-donor of the **HPKIH** and **HAPIH** hydrazones with an *S*-atom leading to the thiohydrazone (**HPKTBH**)²⁷ and thiosemicarbazone (**HDp44mT**)^{28–30} families of chelators (Chart 1).

In the current investigation, we have assessed a series of dithiocarbazate Schiff base analogues (Chart 2) in their reactions with Fe. The ligands share the same *NNS*, tridentate donor set as the **HDp44mT** and **HPKTBH** analogues, but the terminal substituent is a mercaptomethyl or mercaptobenzyl group rather than an amine or aromatic ring. Dithiocarbazate Schiff bases are well described and a number of transition metal complexes are known^{31–41} and these compounds have shown a wide spectrum of biological activity. Little is known about the Fe coordination chemistry of these dithiocarbazate Schiff base ligands^{42,43} and given the resemblance to the highly active thiosemicarbazone Fe chelators we have studied previously,^{21,28–30} this was the focus of the current work. Of particular interest are the relationships between chelator structure, redox properties of the Fe complex and the biological activity (including anti-proliferative efficacy). Modification of the substituents adjacent to the donor group is known to have a marked effect on redox potentials in compounds from the heterocyclic thiosemicarbazone^{28–30} and

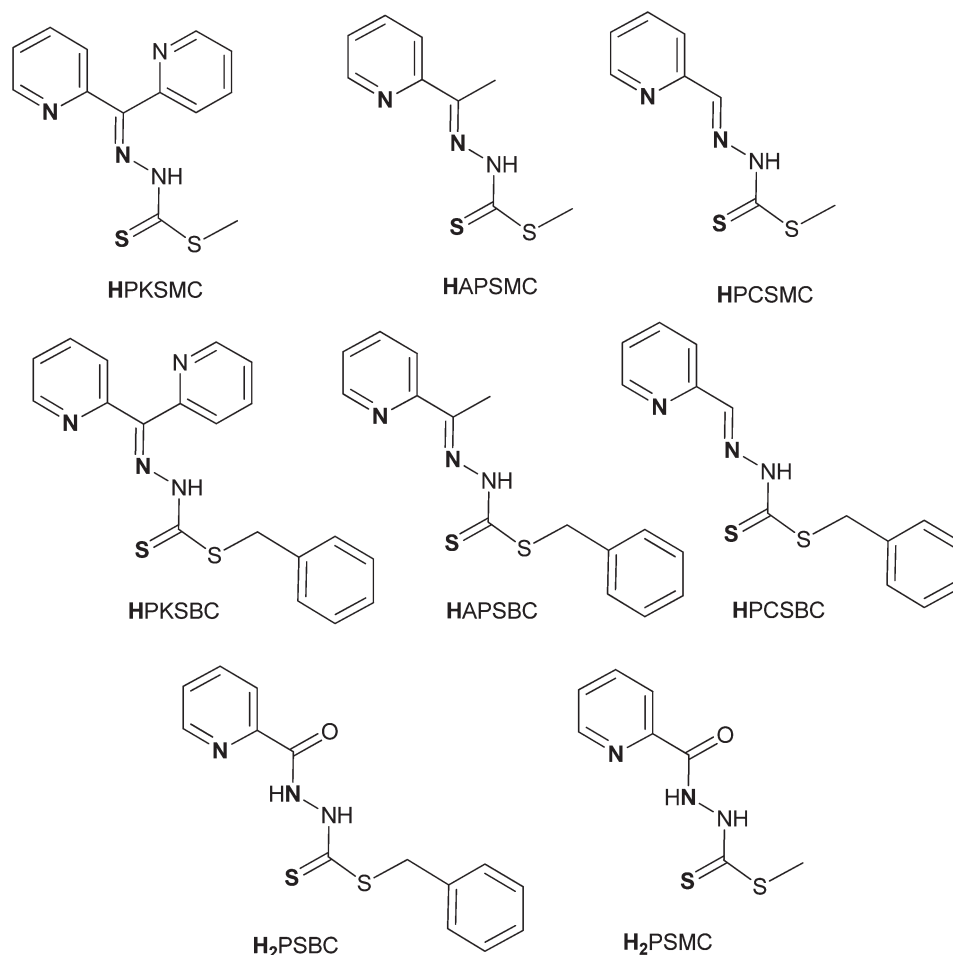


Chart 2 Dithiocarbazate Schiff base ligands investigated in this work and related ligands. Donor atoms are in bold type.

hydrazone^{16–18} series due to extended conjugation along the ligand backbone. Replacement of the terminal amino group with a thioether brings about both differences in inductive and resonance effects, which then are communicated to the coordinated metal ion. In this contribution, we investigate the Fe coordination chemistry of these dithiocarbazate ligands, their effectiveness at mobilising intracellular Fe and their anti-proliferative activity.

Experimental

Safety note

Perchlorate salts are potentially explosive. Although we experienced no problems with the compounds described below they should never be heated in the solid state or scraped from sintered glass frits.

Reagents

S-Methyldithiocarbazate,⁴⁴ and *S*-benzyldithiocarbazate⁴⁵ were prepared according to literature syntheses. All other reagents were obtained commercially and used without further purification.

Free ligand syntheses

2-Acetylpyridine *S*-methyldithiocarbazate (HAPSMC). A suspension of *S*-methyl dithiocarbazate (6.11 g, 0.05 mol) in 75 mL of isopropanol was heated until it dissolved. This mixture was cooled to room temperature then filtered and the residue was washed with isopropyl alcohol then discarded. The filtrate was treated with 2-acetylpyridine (6.05 g, 0.05 mol) added drop-wise. The mixture was stirred for 24 h at room temperature. The resulting yellow precipitate was filtered off, washed with isopropanol and recrystallised from ethanol to give a yellow crystalline product. Yield (7.3 g, 65%). Microanalysis found C, 48.1; H, 5.0; N, 18.8%; Calculated for C₉H₁₁N₃S₂: C, 48.0; H, 4.9; N, 18.7%. IR: $\bar{\nu}$ (cm⁻¹): 3144m, 2913w, 2114w, 1665w, 1615w, 1568m, 1562m, 1484m, 1460s, 1428s, 1366m, 1336m, 1254vs, 1144w, 115w, 1060vs, 1045m, 990w, 949vs, 886w, 774vs, 734vs, 678m, 642s, 620w, and 562m. ¹H NMR (DMSO-d₆): δ 12.57 (s, 1H, NH), 8.62 (m, 1H, py), 8.07 (m, 1H, py), 7.88 (m, 1H, py), 7.45 (m, 1H, py), 2.52 (s, 3H, S-CH₃), 2.45 (s, 3H, C-CH₃). ¹³C NMR (DMSO-d₆): 12.9, 17.0, 120.3, 124.6, 136.8, 148.8, 151.7, 154.3 and 200.6 ppm.

2-Acetylpyridine *S*-benzyldithiocarbazate (HAPSBC). *S*-Benzyl dithiocarbazate (1.98 g, 0.01 mol) was dissolved in hot absolute ethanol (50 mL). To this solution was added drop-wise

an equimolar amount of 2-acetylpyridine (1.21 g, 0.01 mol). The mixture was heated with stirring for 30 min and allowed to stand at room temperature until the product precipitated. The product was filtered off and washed with ethanol to afford dark yellow crystals. Yield (2.29 g, 76%). Microanalysis found C, 59.5; H, 5.1; N, 14.0%; Calculated for $C_{15}H_{15}N_3S_2$: C, 59.8; H, 5.0; N, 13.9%. IR: $\bar{\nu}$ (cm^{-1}); 3171m, 2969w, 2120w, 1668w, 1600w, 1580m, 1563m, 1489s, 1461vs, 1416s, 1367m, 1338m, 1268s, 1230m, 1146w, 1116m, 1062vs, 990w, 961m, 919w, 889w, 776vs, 720s, 681m, 622vs, 589w, and 566m. 1H NMR (DMSO- d_6): δ 12.61 (s, 1H, NH), 8.59 (m, 1H, py), 8.01 (m, 1H, py), 7.83 (m, 1H, py), 7.25 (m, 1H, py), 7.43–7.27 (m, 5H, Ph), 4.48 (s, 2H, CH_2), 2.45 (s, 3H, CH_3). ^{13}C NMR (DMSO- d_6): 12.9, 37.9, 120.4, 124.6, 127.2, 128.5, 129.3, 136.7, 136.8, 148.8, 152.2, 154.2 and 198.8 ppm.

Di-2-pyridyl ketone S-methylthiocarbamate (HPKSMC). S-Methyl dithiocarbamate (1.22 g, 0.01 mol) was dissolved in ethanol (25 mL) and added to a solution of di-2-pyridyl ketone in ethanol (15 mL). The mixture was refluxed for 1 h and then left to stand overnight at room temperature. The product was filtered off and recrystallised from ethanol to give bright yellow crystals. Yield (2.19 g, 76%). Microanalysis found C, 54.2; H, 4.2; N, 19.8%; Calculated for $C_{13}H_{12}N_4S_2$: C, 54.1; H, 4.2; N, 19.4%. IR: $\bar{\nu}$ (cm^{-1}); 3042w, 2981w, 2910w, 1689w, 1564w, 1584m, 1481m, 1452s, 1416vs, 1327s, 1281m, 1242s, 1130s, 1060vs, 998m, 962vs, 890m, 802s, 733vs, 692s, 693m, 614m, and 589s. 1H NMR ($CDCl_3$): δ 15.28 (s, 1H, NH), 8.78 (m, 1H, py), 8.61 (m, 1H, py), 8.03 (m, 1H, py), 7.82 (m, 2H, py), 7.70 (m, 1H, py), 7.37 (m, 2H, py), 2.65 (s, 3H, SCH_3). ^{13}C NMR ($CDCl_3$): 17.4, 123.9, 124.3, 124.5, 127.2, 137.1, 137.3, 142.1, 148.1, 151.1, 155.4 and 202.3 ppm.

Di-2-pyridyl ketone S-benzylthiocarbamate (HPKSBC). Di-2-pyridyl ketone (1.84 g, 0.01 mol) was dissolved in EtOH (15 mL) and mixed with a hot solution of S-benzyl dithiocarbamate (1.98 g, 0.01 mol) in EtOH (30 mL). The mixture was refluxed for 1 h and then left to stand overnight at room temperature. The product was filtered off and recrystallised from ethanol to obtain yellow crystals. Yield (2.94 g, 80.71%). Microanalysis found: C, 62.6; H, 4.4; N, 15.7%; Calculated for $C_{19}H_{16}N_4S_2$: C, 62.6; H, 4.4; N, 15.3%. IR: $\bar{\nu}$ (cm^{-1}); 3054w, 2083w, 1584m, 1480m, 1451s, 1419s, 1327m, 1281m, 1246m, 1121s, 1053vs, 995m, 961m, 845.w, 802s, 737m, 690s, 639m, 615w, and 591s. 1H NMR ($CDCl_3$): δ 15.33 (s, 1H, NH), 8.81(m, 1H, py), 8.61 (m, 1H, py), 8.03 (m, 1H, py), 7.82 (m, 2H, py), 7.72 (m, 2H, py), 7.45–7.27 (m, 5H, Ph and 1H, py), 4.57 (s, 2H, CH_2). ^{13}C NMR ($CDCl_3$): 39.2, 123.9, 124.4, 124.5, 127.3, 127.4, 128.6, 129.5, 136.2, 137.2, 137.3, 142.2, 148.1, 151.1, 155.2 and 202.5 ppm.

2-Pyridinecarbaldehyde S-methylthiocarbamate (HPCSMC). S-Methylthiocarbamate (6.11 g, 0.05 mol) was suspended in isopropanol (75 mL) and refluxed until it dissolved. The solution was allowed to cool to room temperature and the residue was filtered off, washed with isopropyl alcohol and discarded. The filtrate was treated with 2-pyridinecarbaldehyde (5.35 g, 0.05 mol) added drop-wise and the mixture was stirred for 24 h at room temperature. Then the resultant pale yellow precipitate was filtered, washed with isopropanol then recrystallised from

ethanol to give pale yellow crystals. Yield (7.08 g, 67%). Microanalysis found C, 45.6; H, 4.3; N, 20.1%; Calculated for $C_8H_9N_3S_2$: C, 45.5; H, 4.3; N, 19.9%. IR: $\bar{\nu}$ (cm^{-1}); 3090w, 2773m, 2081w, 1582m, 1529s, 1465s, 1434m, 1311m, 1278vs, 1428s, 1145m, 1106m, 1034vs, 997s, 927s, 875m, 774vs, 725m, 678s, and 596m. 1H NMR (DMSO- d_6): δ 13.44 (s, 1H, NH), 8.62 (m, 1H, py), 8.26 (s, 1H, CH), 7.91 (m, 1H, py), 7.87 (m, 1H, py), 7.44 (m, 1H, py), 2.53 (s, 3H, SCH_3). ^{13}C NMR (DMSO- d_6): 16.8, 120, 124.9, 137, 146.4, 149.8, 152.3, and 199.3 ppm.

2-Pyridinecarbaldehyde S-benzylthiocarbamate (HPCSBC). S-Benzylthiocarbamate (1.98 g, 0.01 mol) was dissolved in 35 mL of absolute ethanol and mixed with 2-pyridinecarbaldehyde (1.08 g, 0.01 mol). The mixture was refluxed for 15 min and allowed to stand for 1 h. The yellow powder which formed was filtered off, washed with ethanol and dried in a vacuum desiccator. It was recrystallised twice from absolute ethanol to obtain light yellow crystals. Yield (2.29 g, 79.9%). Microanalysis found C, 58.3; H, 4.6; N, 14.6%; Calculated for $C_{14}H_{13}N_3S_2$: C, 58.5; H, 4.6; N, 14.6%. IR: $\bar{\nu}$ (cm^{-1}); 2923w, 2794m, 1582w, 1566w, 1533s, 1464s, 1438w, 1366w, 1317s, 1278vs, 1108m, 1044s, 1000m, 928s, 830w, 773vs, 714m, 680s, 633, and 600. 1H NMR (DMSO- d_6): δ 13.49 (s, 1H, NH), 8.60 (m, 1H, py), 8.26 (s, 1H, CH), 7.86 (m, 2H, py), 7.45–7.25 (m, 5H, Ph, 1H, py), 4.49 (s, 2H, CH_2). ^{13}C NMR (DMSO- d_6): 37.7, 120.2, 124.9, 127.3, 128.5, 129.3, 163.5, 137, 146.7, 149.8 and 152.2 ppm.

Fe^{III} complexes

[Fe^{III}(APSMC)₂](ClO₄). HAPSMC (1 g, 4.4 mmol) was dissolved in 15 mL of hot ethanol and then triethylamine (0.617 mL, 4.4 mmol) was added. Solid $Fe(ClO_4)_3 \cdot 6H_2O$ (1.025 g, 2.2 mmol) was added directly to the basic ligand solution with stirring and the mixture was gently refluxed for 30 min. After cooling to room temperature, the resulting solid was filtered off and washed with ethanol (10 mL), followed by diethyl ether (10 mL). It was then dried in a vacuum desiccator and recrystallised from ethanol to give dark brown powder. Yield (1.09 g, 82%). Microanalysis found C, 36.1; H, 3.3; N, 14.2%; Calculated for $C_{18}H_{20}ClFeO_4 N_6S_4$: C, 35.8; H, 3.3; N, 13.9%. IR: $\bar{\nu}$ (cm^{-1}); 3078w, 2926w, 1700w, 1597m, 1481w, 1423s, 1310m, 1148w, 1084vs, 1032vs, 945s, 818m, 774s, 742s, 621s, and 557w. Electronic spectrum (MeCN): 425 nm ($11\ 300\ M^{-1}\ cm^{-1}$), 343 (23 400).

[Fe^{III}(APSBC)₂](ClO₄). HAPSBC (0.7 g, 2.3 mmol) was dissolved in 30 mL of hot ethanol and $Fe(ClO_4)_3 \cdot 6H_2O$ (0.54 g, 1.2 mmol) was added directly to the solution. Et_3N (0.32 mL, 2.3 mmol) was added and the dark brown mixture was refluxed for 30 min. The reaction mixture was filtered while hot to obtain an initial crop of the desired product. The filtrate was allowed to cool at room temperature, and was then put in the refrigerator overnight. The brown precipitate was collected by vacuum filtration and washed with ethanol and diethyl ether to give a second crop. Total yield (0.62 g, 70%). Microanalysis C, 47.6; H, 3.7; N, 11.1%; Calculated for $C_{30}H_{28}ClFe N_6O_4S_4$: C, 47.7; H, 3.7; N, 11.1%. IR: $\bar{\nu}$ (cm^{-1}); 3093w, 1598m, 1492w, 1427vs,

1330m, 1242w, 1170m, 1077vs, 1027vs, 942s, 812w, 785s, 694s, and 620s. Electronic spectrum (MeCN): 428 nm ($8530 \text{ M}^{-1} \text{ cm}^{-1}$), 350 ($25\ 600$).

[Fe^{III}(PCSBC)₂](ClO₄)·1.5H₂O. HPCSBC (0.7 g, 2.4 mmol) was dissolved in 300 mL of hot ethanol and then triethylamine (0.34 mL, 2.4 mmol) was added. Solid Fe(ClO₄)₃·6H₂O (0.54 g, 1.2 mmol) was added to the basic ligand solution with stirring and the mixture was gently refluxed for 1 h. The reaction mixture was cooled to room temperature and the resulting crude dark brown solid containing a mixture of compounds was filtered off, washed with 10 mL of ethanol followed by 10 mL of diethyl ether. A column of dry silica (100 × 32 mm diameter, Scharlau or Merck Silica gel 60, 230–400 mesh) was prepared. The crude product (0.3 g) was dissolved in CH₃CN (~50 mL) and adsorbed onto Celite (~1.3 g) by evaporation to dryness on a rotary evaporator at room temperature (see Safety Note). The resulting solids were packed dry onto the column which was tapped gently to remove air pockets. The column was eluted with a step-wise gradient of CH₃CN–DCM starting with 0.1% CH₃CN–DCM with the application of air pressure. A green band of [Fe^{II}(PCSBC)₂] began to elute with 5% CH₃CN–DCM. The polarity of the solvent mixture was gradually increased until all of this compound had eluted. This compound was characterised separately (see Fe^{II} complex section below). The brown second component ([Fe^{III}(PCSBC)₂](ClO₄)) began to elute with 25% CH₃CN–DCM. Evaporation to dryness at room temperature gave the product as a brown solid. Yield (0.4 g, 43%). Microanalysis found C, 44.76; H, 3.62; N, 10.77%; Calculated for C₂₈H₂₇ClFeO_{5.5}N₆S₄: C, 44.5; H, 3.6; N, 11.1%. IR: $\bar{\nu}$ (cm⁻¹); 3029w, 2922w, 1602m, 1579m, 1477w, 1404s, 1342m, 1219w, 1066vs, 974s, 910m, 883w, 680m, 619s, and 563w. Electronic spectrum (MeCN): 434 nm ($8130 \text{ M}^{-1} \text{ cm}^{-1}$), 352 ($23\ 800$).

[Fe^{III}(PCSMC)₂](ClO₄). HPCSMC (1 g, 4.7 mmol) was dissolved in 75 mL of hot ethanol and solid Fe(ClO₄)₃·6H₂O (0.54 g, 2.4 mmol) was added directly to the solution. Triethylamine (0.66 mL, 4.7 mmol) was added to the dark brown mixture which was gently refluxed for 30 min. The reaction mixture was filtered while still hot to obtain an initial crop of dark brown compound. The filtrate was allowed to cool at room temperature and then refrigerated overnight. A second crop was obtained by vacuum filtration and was washed with ethanol and diethyl ether. Attempts to recrystallise the complex were unsuccessful. Column chromatography (as described in the previous synthesis) enabled separation of [Fe^{II}(PCSMC)₂] (green, first band) from the desired product [Fe^{III}(PCSMC)₂](ClO₄) which was evaporated to dryness at room temperature (see Safety Note) to afford a brown solid. Yield (0.68 g, 50%). Microanalysis found C, 33.75; H, 2.90; N, 14.32%; Calculated for C₁₆H₁₆ClFeO₄N₆S₄: C, 33.37; H, 2.80; N, 14.59%. IR: $\bar{\nu}$ (cm⁻¹); 3098w, 1603m, 1477w, 1405vs, 1344m, 1306m, 1216m, 1166w, 1062s, 978s, 914w, 766m, and 619s. Vapour diffusion of diethyl ether into an acetone solution of the complex afforded crystals suitable for X-ray work. Electronic spectrum (MeCN): 431 nm ($9370 \text{ M}^{-1} \text{ cm}^{-1}$), 356 ($20\ 100$).

[Fe^{III}(PCSMC)(PSMC)]·2Me₂CO·4H₂O. HPCSMC (1 g, 4.7 mmol) was dissolved in 100 mL of hot ethanol and then triethylamine (0.66 mL, 4.7 mmol) was added to the solution.

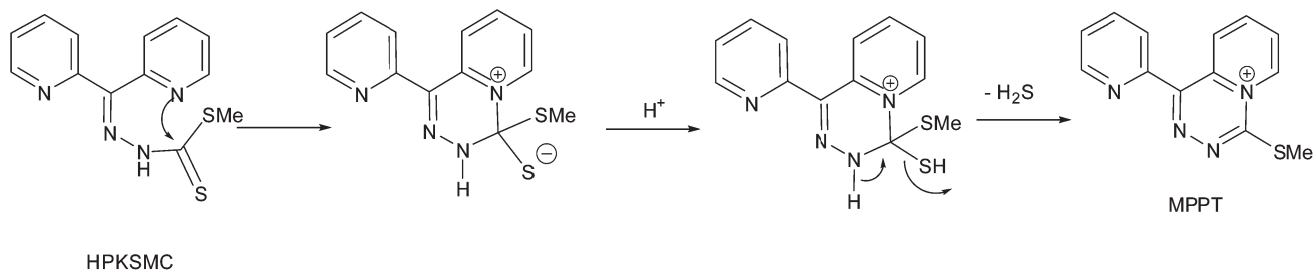
Solid Fe(ClO₄)₃·6H₂O (1.08 g, 2.41 mmol) was added to the basic ligand solution with stirring and the mixture was gently refluxed for 1 h. On cooling to room temperature the resulting crude dark brown solid was filtered off and washed with 10 mL of ethanol followed by 10 mL of diethyl ether. Column chromatography on silica (see previous synthesis) was carried out using a solvent gradient of CH₃OH (in increasing quantities) in DCM. After elution of a green band of [Fe^{II}(PCSMC)₂], the desired mixed-ligand complex [Fe^{III}(PCSMC)(PSMC)] eluted. This was evaporated to dryness. Yield 50%. The complex was recrystallised with acetone–diethyl ether. Microanalysis found C, 38.6; H, 4.1; N, 12.1%; calculated for C₂₂H₃₅FeN₆O₇S₄: C, 38.9; H, 5.2; N, 12.4%. IR: $\bar{\nu}$ (cm⁻¹); 3401m, 2921m, 1583vs, 1371s, 1283m, 1192w, 1073vs, 995m, 916m, 761, 686w, and 620m. Crystals suitable for crystallography were obtained by slow diethyl ether vapour diffusion into a concentrated acetone solution. Electronic spectrum (MeCN): 618 nm ($1440 \text{ M}^{-1} \text{ cm}^{-1}$), 441 (3850), 300 ($11\ 300$).

[Fe^{III}(PKSMC)₂](ClO₄). HPKSMC (0.8 g, 2.8 mmol) was dissolved in 30 mL of hot ethanol and (0.64 1.4 mmol) of solid Fe(ClO₄)₃·6H₂O was added directly to the solution. Et₃N (0.39 mL, 2.8 mmol) was added to the dark brown mixture which was gently refluxed for 30 min. The reaction mixture was filtered while still hot to obtain an initial crop. The filtrate was allowed to cool at room temperature and refrigerated overnight. The dark brown product was collected by vacuum filtration and washed with ethanol and diethyl ether to give a second batch of brown solid. Yield (0.83 g, 83%). Microanalysis found C, 43.0; H, 3.2; N, 15.4%; Calculated for C₂₆H₂₂ClFeN₈O₄S₄: C, 42.8; H, 3.0; N, 15.4%. IR: $\bar{\nu}$ (cm⁻¹); 3090w, 1620m, 1584m, 1529w, 1413s, 1340s, 1313m, 1159m, 1073vs, 1000s, 821w, 792m, 743s, and 615vs. Crystals of [Fe^{III}(PKSMC)₂](ClO₄)₂ (MPPT being a triazinium product of HPKSMC desulfuration, see Scheme 1) suitable for X-ray work were obtained from diethyl ether vapour diffusion into a concentrated acetone solution of the crude first crop. Electronic spectrum (MeCN): 445 nm ($12\ 100 \text{ M}^{-1} \text{ cm}^{-1}$), 362 ($27\ 000$).

[Fe^{III}(PKSBC)₂](ClO₄)·2.5H₂O. HPKSBC (0.8 g, 2.2 mmol) was dissolved in 65 mL of hot ethanol and solid Fe(ClO₄)₃·6H₂O (0.51 g, 1.1 mmol) was added directly to the solution. Triethylamine (0.31 mL, 2.2 mmol) was added to the dark brown mixture which was gently refluxed for 30 min. The reaction mixture was filtered while still hot and the filtrate was allowed to cool at room temperature and refrigerated overnight. The dark brown product was collected by vacuum filtration and washed with diethyl ether. Yield (0.46 g, 48%). Microanalysis found C, 49.3; H, 3.6; N, 12.3%; Calculated for C₃₈H₃₅ClFeN₈O_{6.5}S₄: C, 49.2; H, 3.8; N, 12.1%. IR: $\bar{\nu}$ (cm⁻¹); 3059w, 1585m, 1494w, 1408vs, 1335s, 1243w, 1074vs, 989s, 820w, 745m, 700m, and 617vs. Electronic spectrum (MeCN): 431 nm ($9370 \text{ M}^{-1} \text{ cm}^{-1}$), 356 ($20\ 100$).

Fe^{II} complexes

The Fe^{II} complexes were synthesised by the following general method. 2.4 mmol of the appropriate dithiocarbamate ligand was dissolved in ethanol (30–150 mL) and the mixture was purged



Scheme 1

with nitrogen for 10 min. Et₃N (0.34 mL, 2.4 mmol) was added followed by solid Fe(ClO₄)₂·6H₂O (0.44 g, 1.2 mmol) with stirring. The mixture was gently refluxed for 30 min under nitrogen. Upon cooling, the green product was filtered off and washed with 10 mL of ethanol followed by 10 mL diethyl ether.

[Fe^{II}(APSMC)₂]·H₂O. Yield (0.93 g, 80%). Microanalysis found C, 41.0; H, 3.9; N, 15.9%; Calculated for C₁₈H₂₂FeN₆S₄: C, 41.4; H, 4.2; N, 16.1%. IR: $\bar{\nu}$ (cm⁻¹); 3414b, 2927w, 1629w, 1589m, 1467w, 1395s, 1322vs, 1140m, 1093m, 1030vs, 933m, 816w, 738s, 647w, 627m, and 556w. Electronic spectrum (MeCN): 676 nm (7360 M⁻¹ cm⁻¹), 429 (sh, 15 100), 331 (28 300).

[Fe^{II}(APSBC)₂]·2H₂O. Yield (0.58 g, 72%). Microanalysis found C, 51.4; H, 4.2; N, 12.4%; Calculated for C₃₀H₃₂FeN₆O₂S₄: C, 52.0; H, 4.7; N, 12.1%. IR: $\bar{\nu}$ (cm⁻¹); 3395b, 1627w, 1590s, 1400vs, 1323vs, 1286m, 1234w, 1142m, 1092m, 1031vs, 942s, 765s, 694s, 630m, and 567. Electronic spectrum (MeCN): 679 nm (5920 M⁻¹ cm⁻¹), 429 (sh, 12 500), 333 (26 300).

[Fe^{II}(PCSMC)₂]·2H₂O. Yield (0.95 g, 81%). Microanalysis found C, 37.9; H, 3.5; N, 16.0%; Calculated for C₁₆H₂₀FeN₆O₂S₄: C, 37.5; H, 3.9; N, 16.4%. IR: $\bar{\nu}$ (cm⁻¹); 3374b, 2970w, 2111m, 1594s, 1495m, 1463w, 1429vs, 1372vs, 1322m, 1204m, 1105m, 1049vs, 953s, 882m, 844m, 754s, 666w, and 566m. Electronic spectrum (MeCN): 684 nm (7210 M⁻¹ cm⁻¹), 441 (sh, 7210), 346 (17 800).

[Fe^{II}(PCSBC)₂]·0.5H₂O. Yield (0.4 g, 52%). Microanalysis found C, 52.7; H, 4.0; N, 12.9%; Calculated for C₂₈H₂₅FeN₆O₅S₄: C, 52.7; H, 4.0; N, 13.2%. IR: $\bar{\nu}$ (cm⁻¹); 3374b, 2970w, 2111m, 1594s, 1495m, 1463w, 1429vs, 1372vs, 1322m, 1204m, 1105m, 1049vs, 953s, 882m, 844m, 754s, 666w, and 566m. Electronic spectrum (MeCN): 664 nm (6320 M⁻¹ cm⁻¹), 429 (sh, 10 500), 331 (28 400).

[Fe^{II}(PKSMC)₂]·1.5H₂O. Yield (0.8 g, 70%). Microanalysis found C, 47.4; H, 3.8; N, 16.7%; Calculated for C₂₆H₂₅FeN₈O_{1.5}S₄: C, 47.5; H, 3.8; N, 17.0%. IR: $\bar{\nu}$ (cm⁻¹); 3059w, 2083w, 1595s, 1496s, 1394vs, 1333m, 1287m, 1207.61m, 1153w, 1108s, 1040s, 968w, 852m, 759s, 699s, and 561w. Electronic spectrum (MeCN): 682 nm (6320 M⁻¹ cm⁻¹), 445 (sh, 10 500), 344 (25 300).

Fe^{II}(PKSBC)₂]·0.5H₂O. Yield (0.5 g, 64%). Microanalysis found C, 57.5; H, 3.9; N, 14.4%; Calculated for C₃₈H₃₁FeN₈O_{0.5}S₄: C, 57.6; H, 4.0; N, 14.2%. IR: $\bar{\nu}$ (cm⁻¹);

3063w, 2119w, 1581m, 1481m, 1379vs, 1322s, 1239w, 1112w, 1061vs, 1015w, 980vs, 858w, 785s, 766m, 740s, 699m, 601s, and 556w. Electronic spectrum (MeCN): 684 nm (7120 M⁻¹ cm⁻¹), 441 (sh, 8000), 331 (17 800).

Physical methods

UV-vis spectra were recorded on a Perkin Elmer Lambda 40 spectrophotometer. Solutions were analysed immediately before any redox reactions occurred. This was particularly important for the Fe^{II} complexes which slowly oxidised in aerated solutions. IR spectra were recorded as undiluted solids on a Perkin Elmer 1600 FTIR spectrometer in attenuated total reflectance mode. NMR spectra were acquired on a Bruker Avance 300 MHz spectrometer and all resonances were given relative to tetramethylsilane (δ = 0 ppm). Cyclic voltammetry was recorded with a BAS100B/W potentiostat employing a glassy carbon working electrode, Pt wire counter and Ag–AgCl reference electrode. The solvent was MeCN–H₂O (7 : 3) and the supporting electrolyte was 0.1 M Et₄NClO₄. All solutions were purged with N₂ before measurement. Approximately 1 mM solutions of analyte were used.

Biological assays

Cell culture. The chelators were dissolved to make 10 mM stock solutions in DMSO and diluted in medium containing 10% foetal calf serum (Commonwealth Serum Laboratories, Melbourne, Australia). A final [DMSO] < 0.5% (v/v) was used to ensure that DMSO had no effect on proliferation, ⁵⁹Fe uptake, or ⁵⁹Fe mobilisation from cells.⁴⁶ The human SK-N-MC neuroepithelioma cell line (American Type Culture Collection, Manassas, VA) was grown using standard procedures²⁷ in a humidified atmosphere of 5% CO₂–95% air at 37 °C in an incubator (Forma Scientific, Marietta, OH).

Effect of the chelators on cellular proliferation

The effect of the chelators on cellular proliferation was determined using the [3-(4,5-dimethylthiazol-2-yl)-2,5-diphenyltetrazolium] (MTT) assay *via* standard methods.^{27,46} The SK-N-MC cell line was seeded at 1.5 × 10⁴ cells per well in 96-well microtiter plates in medium containing the Fe uptake protein, human ⁵⁹Fe₂-transferrin (Fe₂-Tf; 1.25 μM) and chelators at a range of concentrations (0–25 μM). The control samples contained medium with Fe₂-Tf (1.25 μM) in the absence of the ligands.

Table 1 Crystal data

	HAPSMC	[Fe(PCSMC) ₂](ClO ₄)	[Fe(PKSMC) ₂](MPPT)(ClO ₄) ₂	[Fe(PSMC)(PCSMC)]·Me ₂ CO
Formula	C ₉ H ₁₁ N ₃ S ₂	C ₁₆ H ₁₆ ClFeN ₆ O ₄ S ₄	C ₃₉ H ₃₃ Cl ₂ FeN ₁₂ O ₈ S ₅	C ₁₉ H ₂₁ FeN ₆ O ₂ S ₄
Mol. Wt	225.33	575.89	1084.82	549.51
Crystal system	Triclinic	Monoclinic	Triclinic	Trigonal
<i>a</i> (Å)	5.8633(5)	33.437(2)	7.9883(3)	36.376(5)
<i>b</i> (Å)	8.148(1)	8.8580(4)	14.5465(7)	
<i>c</i> (Å)	11.757(2)	14.865(1)	20.3055(9)	9.3420(7)
α (°)	81.91(1)		89.484(4)	
β (°)	79.334(9)	90.851(5)	82.777(4)	
γ (°)	84.497(8)		84.060(4)	
<i>V</i> (Å ³)	545.1(1)	4402.4(4)	2328.2(2)	10 705(2)
λ (Å)	0.71073	0.71073	1.54184	0.71073
<i>T</i> (K)	293	293	293	293
<i>Z</i>	2	8	2	18
Space group	<i>P</i> $\bar{1}$	<i>C</i> 2/ <i>c</i>	<i>P</i> $\bar{1}$	<i>R</i> $\bar{3}$
μ (mm ⁻¹)	0.452	1.224	6.302	1.014
Total refs	3488	14 700	21 135	8404
Indep. refs (<i>R</i> _{int})	1905 (0.0292)	3881 (0.0425)	7365 (0.0398)	4169 (0.0729)
<i>R</i> ₁ (obs. data)	0.0432	0.0406	0.0424	0.0933
w <i>R</i> ₂ (all data)	0.0826	0.0908	0.1120	0.2546

The cells were then incubated in a humidified atmosphere containing 5% CO₂ and 95% air at 37 °C for 72 h. Subsequently, 10 μ L of MTT (5 mg mL⁻¹) was added to each well and incubated at 37 °C for 2 h. The cells were solubilised with 100 μ L of 10% SDS–50% isobutanol in 10 mM HCl and the plates were then read at 570 nm using a scanning multi-well spectrophotometer. The inhibitory concentration (IC₅₀) was defined as the chelator concentration needed to decrease the absorbance to 50% of the untreated control. Absorbance was shown to be directly proportional to cell counts, as shown previously.⁴⁶

Preparation of ⁵⁶Fe- and ⁵⁹Fe-Tf

Human Tf (Sigma) was labelled with either ⁵⁶Fe or ⁵⁹Fe (Dupont NEN, MA) to produce ⁵⁶Fe₂-Tf and ⁵⁹Fe₂-Tf, respectively, as described previously.^{47,48} Any unbound ⁵⁹Fe was removed by passage through a Sephadex G25 column and exhaustive vacuum dialysis against an excess of 0.15 mM NaCl buffered to pH 7.4 with 1.4% NaHCO₃ *via* standard methods.⁴⁷

Effect of chelators on ⁵⁹Fe efflux from SK-N-MC cells

The ability of the chelators to mobilise ⁵⁹Fe from SK-N-MC cells was performed by established techniques.⁴⁶ After prelabelling cells with ⁵⁹Fe₂-Tf (0.75 μ M) for 3 h at 37 °C, the cell monolayer was washed four times on ice with ice-cold PBS and subsequently incubated with the chelators (25 μ M) for 3 h at 37 °C. The overlying media containing released ⁵⁹Fe was separated from the cells using a Pasteur pipette. Radioactivity in the cell pellet and the supernatant was measured using a γ -scintillation counter (Wallac Wizard 3, Turku, Finland). In these studies, the novel ligands were compared to the well-characterised chelators, DFO, H₂NIH (311) and HDp44mT.^{19,46,47}

Effect of chelators at preventing ⁵⁹Fe uptake from ⁵⁹Fe₂-Tf by SK-N-MC cells

The ability of the novel ligands to prevent cellular ⁵⁹Fe uptake from the Fe transport protein, ⁵⁹Fe₂-Tf, was examined *via*

established methods.⁴⁶ Cells were incubated with ⁵⁹Fe₂-Tf (0.75 μ M) for 3 h at 37 °C in the presence of the chelators (25 μ M). The cells were washed on ice four times with ice-cold PBS and the internalised ⁵⁹Fe was determined by standard procedures by incubating the monolayer for 30 min at 4 °C with the protease, Pronase (1 mg mL⁻¹; Sigma).^{46,47} The cells were removed using a plastic spatula and centrifuged at 14 000 rpm for 1 min. The pronase-insensitive fraction represents internalised ⁵⁹Fe, while the supernatant represents the membrane-bound, pronase-sensitive ⁵⁹Fe that was released by the protease.^{46,47} The ligands were compared to the previously characterised chelators, DFO, 311 and HDp44mT.^{19,46}

Crystallography

Crystallographic data were acquired at 23 °C on an Oxford Diffraction Gemini CCD diffractometer employing either Mo-K α or Cu-K α radiation (see Table 1) and operating in the ω -scan mode. Data reduction and empirical absorption corrections (multi-scan) or analytical absorption corrections were performed with Oxford Diffraction CrysAlisPro software. Structures were solved by direct methods with SHELXS and refined by full-matrix least-squares analysis with SHELXL-97.⁴⁹ All non-H atoms were refined with anisotropic thermal parameters. Molecular structure diagrams were produced with ORTEP3.⁵⁰ All calculations were carried out within the WinGX graphical user interface.⁵¹ In the structure of [Fe(PCSMC)(PSMC)]·Me₂CO the acetone molecule was modelled as a diffuse contribution to the overall scattering without specific atom positions using SQUEEZE/PLATON.⁵² Crystal and refinement data are summarised in Table 1.

Results and discussion

Free ligand characterisation

The dithiocarbazate Schiff base ligands in Chart 2 were prepared by variations on published procedures^{31,33} involving condensation between *S*-methyl (or *S*-benzyl) thiocarbazate and the corresponding aldehyde or ketone. These Schiff base ligands

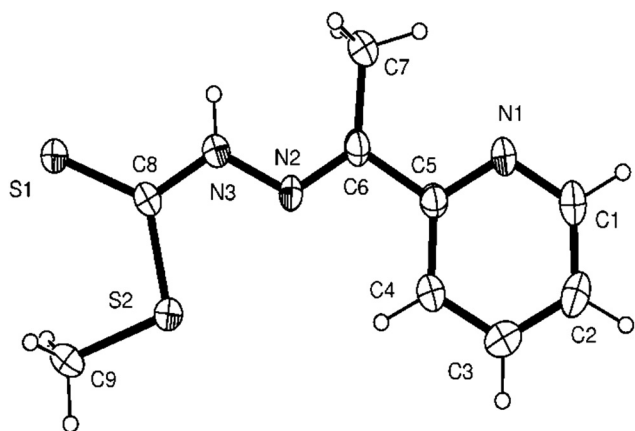


Fig. 1 ORTEP view of the free ligand **HAPSMC** (30% probability ellipsoids).

present a homologous series bearing a common *NNS* donor set. As a representative example, the single crystal structure of **HAPSMC** was determined. A view of the ligand appears in Fig. 1. The compound adopts an approximately planar conformation. Of note is that the donor atoms (N1, N2 and S1) are not in the required conformation for tridentate coordination and 180° rotation of the C8–N3 and C5–C6 bonds are required. The C8–S1 bond has double bond character in contrast to the *S*-methyl single bond (S2–C9). The C8–S2 bond is slightly shorter than S2–C9 indicating some electronic delocalisation. Selected bond lengths appear in Table 2.

Fe complexation

Deprotonation of the thioamide N atom accompanies tridentate coordination of each dithiocarbamate Schiff base ligand. The Fe complexes of these ligands were the focus of our investigation here. Given the parallels with our previous work on the **HPCIH** (hydrazone)¹⁶ and **HDp44mT** (thiosemicarbazone) series,²⁸ the present set of dithiocarbamate compounds exhibit chemical and biological properties reminiscent of both. The Fe^{II} complexes were prepared by reaction of the ligands with ferrous perchlorate in EtOH under an inert atmosphere to avoid oxidation to the

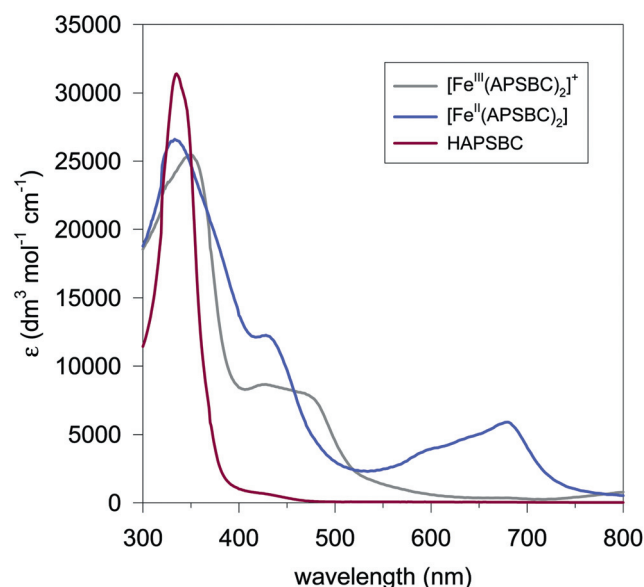


Fig. 2 UV-vis spectra of **HAPSMC** and its Fe^{II} and Fe^{III} complexes measured in MeCN.

trivalent state during synthesis. Each ferrous complex exhibited a characteristically green colour due to a broad and intense MLCT (Fe^{II} → pyridine) transition around 670 nm (Fig. 2). Similar maxima have been identified in the Fe^{II} complexes of the **HPCIH**^{16–18} and **HDp44mT**^{28–30} analogues. In the solid state, the Fe^{II} complexes are stable and do not undergo oxidation. The Fe^{III} complexes were prepared by direct reaction with ferric perchlorate in EtOH. The ferric complexes are dark brown and exhibit a series of broad, overlapping and intense electronic transitions that span most of the visible region (Fig. 2). The free ligands exhibit no electronic maxima in the visible region and are pale yellow in colour.

Purification of the Fe complexes was generally possible by recrystallisation, but column chromatography (silica) was sometimes necessary to separate mixtures of Fe^{II} and Fe^{III} complexes that co-precipitated. This is a new method for purification of these complexes and facilitated isolation of compounds for single crystal X-ray work.

Table 2 Selected bond lengths and angles (ligands 'a' and 'b' defined by labels in Fig. 3 and 4). For the heteroligand complex [Fe(PSMC)(PCSMC)] bonds to the oxidised PSMC²⁻ ligand are in italics

	HAPSMC	[Fe(PCSMC) ₂] ⁺ , Ligand a, b	[Fe(PKSMC) ₂] ⁺ , Ligand a, b	[Fe(PSMC)(PCSMC)], <i>PSMC, PCSMC</i>
C8–S1	1.645(3)	1.720(3), 1.713(3)	1.735(3), 1.735(3)	<i>1.73(1), 1.751(9)</i>
C8–S2	1.762(3)	1.710(3), 1.713(3)	1.738(3), 1.733(3)	<i>1.765(9), 1.740(9)</i>
C8–N3	1.333(3)	1.282(4), 1.288(4)	1.291(4), 1.301(4)	<i>1.29(1), 1.26(1)</i>
C9–S2	1.791(3)	1.764(3), 1.767(4)	1.794(4), 1.796(4)	<i>1.75(1), 1.78(1)</i>
N2–N3	1.374(3)	1.368(3), 1.371(3)	1.384(3), 1.385(3)	<i>1.365(9), 1.369(9)</i>
N2–C6	1.282(3)	1.277(3), 1.277(3)	1.308(4), 1.309(4)	<i>1.38(1), 1.27(1)</i>
Fe–N1a/b	—	1.968(2), 1.956(3)	1.984(3), 1.984(2)	<i>1.992(6), 1.990(7)</i>
Fe–N2a/b	—	1.880(2), 1.879(2)	1.910(2), 1.912(2)	<i>1.911(7), 1.942(7)</i>
Fe–S1a/b	—	2.1891(9), 2.201(1)	2.2255(9), 2.2273(9)	<i>2.223(2), 2.265(3)</i>
N1a/b–Fe–N2a/b	—	80.9(1), 80.5(1)	80.4(1), 80.4(1)	<i>81.6(3), 79.7(3)</i>
N2a/b–Fe–S1a/b	—	84.97(7), 85.03(8)	85.37(8), 85.56(8)	<i>84.8(2), 82.8(2)</i>
N2a–Fe–N2b	—	176.5(1)	177.8(1)	<i>176.5(3)</i>

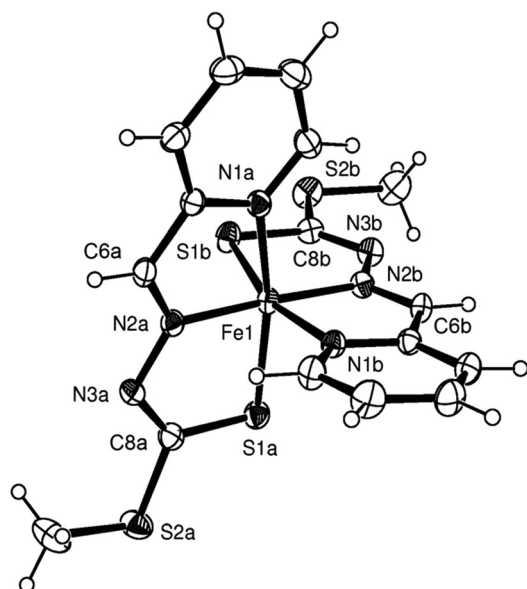


Fig. 3 ORTEP view of the $[\text{Fe}(\text{PCSMC})_2]^+$ cation (30% probability ellipsoids).

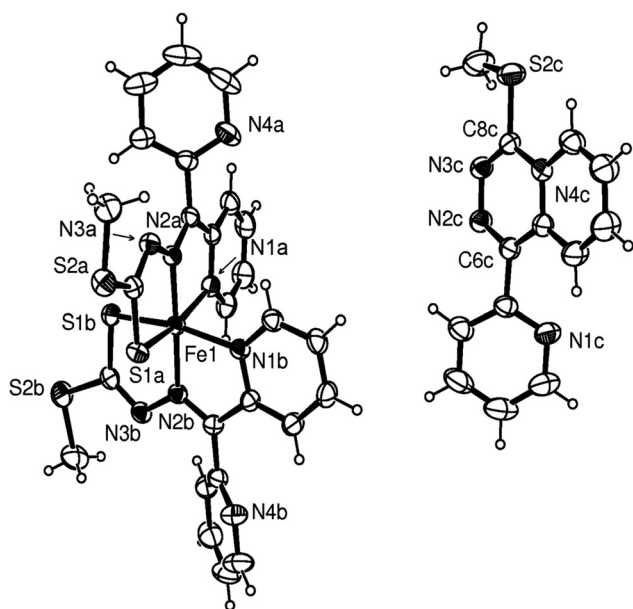


Fig. 4 ORTEP view of the $[\text{Fe}(\text{PKSMC})_2]^+$ (left) and MPPT^+ (right) cations (30% probability ellipsoids).

The crystal structure of $[\text{Fe}(\text{PCSMC})_2](\text{ClO}_4)$ was determined. A view of the complex cation appears in Fig. 3. The meridional configuration of each ligand is apparent to produce a complex with approximate C_2 symmetry. The Fe–N and Fe–S bond lengths (Table 2) are characteristic of low spin Fe^{III} complexes seen in related thiosemicarbazone and thiohydrazone ferric complexes from the **HDp44mT**³⁰ and **HPKTBH**²⁷ series. There is no conformational flexibility in the complex cation except for the *S*-methyl groups which each adopt an *anti*-conformation with respect to the adjacent coordinated *S*-donor. The most significant variations in intraligand bond lengths (going from free ligand to

complex) are in the region of the coordinated *S*-donors. The C8–S1 and C8–S2 bond lengths in $[\text{Fe}(\text{PCSMC})_2]^+$ are identical in the complex due to electron delocalisation across the N3–C8 (S1)–S2 moiety in contrast to what is seen in the structure of the analogue **HAPSMC** where the C8=S1 bond has definite double bond character. The C3–N3 bonds in each ligand shorten appreciably upon complexation, defining an effective imine-thiolate ($-\text{N}=\text{C}-\text{S}^-$) resonance form of the coordinated ligand anion. No significant variations in the N2–N3 or N2–C6 bonds are apparent on deprotonation and complexation.

The crystal structure of the homologous complex $[\text{Fe}(\text{PKSMC})_2]^+$ was also determined (Fig. 4). The geometry of the complex cation mirrors that of $[\text{Fe}(\text{PCSMC})_2]^+$. Again the coordinate bonds and angles are consistent with low spin Fe^{III} complexes of the dithiocarbazate Schiff base ligands (Table 2) but the Fe–N and Fe–S bonds are slightly longer than seen in $[\text{Fe}(\text{PCSMC})_2]^+$. This may be attributed to a combination of interligand repulsion brought about by introduction of the non-coordinating pyridyl rings and also electron-withdrawing effects of these groups that may slightly weaken the donor strength of the PKSMC^- ligand.

Curiously, the complex $[\text{Fe}(\text{PKSMC})_2]^+$ co-crystallised with a cationic pyridotriazinium derivative (MPPT^+ , Fig. 4); a by-product of ligand desulfuration. It is not known whether Fe catalyses this reaction, although the loss of sulfide (or hydrogen sulfide) is probably assisted by the presence of free metal ions. A tentative mechanism is proposed in Scheme 1. It is known that elimination of methanethiol followed by ring closure is an alternative possibility in dithiocarbazates of this type, leading to an exocyclic thioamide (rather than thioether) group.⁵³

Depending on the order of addition of reagents (ligand, ferric perchlorate and base), different products were observed in the synthesis of the Fe^{III} complex of **HPCSMC**. When the ferric salt was added last, an unusual mixed-ligand Fe^{III} complex was obtained following column chromatography, namely $[\text{Fe}(\text{PCSMC})(\text{PSMC})]$. The ligand dianion PSMC^{2-} (Chart 2) is

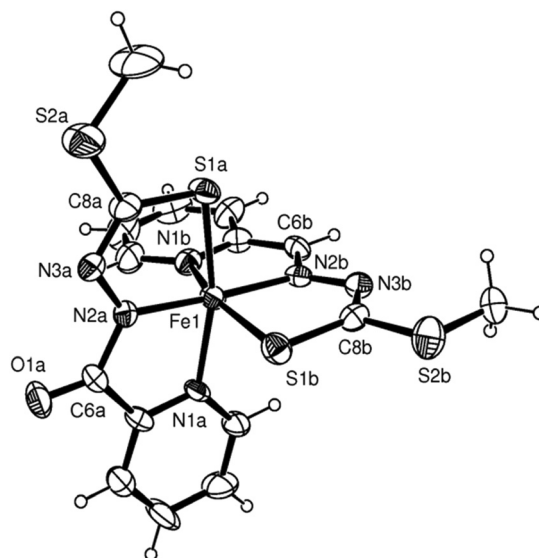


Fig. 5 ORTEP view of $[\text{Fe}(\text{PCSMC})(\text{PSMC})]$ (30% probability ellipsoids).

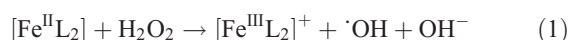
effectively a hydroxylated derivative of PCSMC⁻. The Fe^{III} complex, [Fe(PCSMC)(PSMC)] exhibited some characteristic spectroscopic features, including an intense C=O vibrational band in the IR spectrum (1583 cm⁻¹), which was absent in all other IR spectra reported here.

The structure of the complex was confirmed by X-ray crystallography. A view of the neutral complex [Fe(PCSMC)(PSMC)] is shown in Fig. 5. The presence of O1a on the PSMC²⁻ ligand is apparent. This has some important structural influences on the complex and particularly on the PCSMC⁻ co-ligand. The Fe–N2b and Fe–S1b bonds lengthen considerably in comparison with the symmetrical [Fe(PCSMC)₂]⁺ and [Fe(PKSMC)₂]⁺ complexes. This may be partially attributed to a *trans* influence of the dianionic PSMC²⁻ ligand. The Fe–N2b bond (from PCSMC⁻) is *trans* to the Fe–N2a bond (from PSMC²⁻) where N2a formally carries a negative charge due to amide deprotonation. The extension of the Fe–S1b bond may be a consequence of Fe–N1b elongation as both donor atoms are part of the same rigid chelate ring. Another structural feature is the change in bond order of C6–N2 from a formal (imine) double bond in the dithiocarbazates (Table 2), to an intermediate bond order closer to one (C6a–N2a 1.38(1) Å) characteristic of a deprotonated amide in PSMC²⁻.

Ligand hydroxylation of this kind is unusual but not without precedent. Our previous work has uncovered other Schiff base ligands derived from 2-pyridinecarbaldehyde which undergo Fe^{III} catalysed oxidation reactions^{34,54} leading to hydrazine (as opposed to hydrazone) analogues (the H₂IPH analogues, Chart 1). The mechanism of this reaction is very complicated,³⁹ but nucleophilic attack by water on the C6=N2 double bond followed by ligand dehydrogenation are involved. The oxidant is Fe^{III} and not dioxygen. The properties of Fe complexes from the H₂IPH series are very different, and in fact, only Fe^{III} complexes have been isolated in contrast to the Fe^{II} complexes from the corresponding HPCIH series.

Redox properties

The Fe^{III/II} redox potentials are an important determinant of biological activity and affinity for Fe in each of its oxidation states. Complexes with exceptionally high redox potentials will be most stable in the Fe^{II} form under biological conditions, while those with low (large negative) redox potentials will be spontaneously oxidised to Fe^{III}. Between these extremes, both Fe^{III} and Fe^{II} may co-exist and interconvert. This is germane in a cellular environment due to the ability of redox-active Fe complexes to catalyse the production of hydroxyl radicals (Fenton chemistry, eqn (1)),⁵⁵ which leads to oxidative stress and damage to important biomolecules.



Previous investigations on Fe complexes of thiosemicarbazone complexes^{28–30} have shown that compounds possessing Fe^{III/II} redox potentials in the range 0 to +200 mV vs. NHE are also able to catalyse the production of hydroxyl radicals in the presence of hydrogen peroxide. For eqn (1) to be catalytic, the Fe^{III}

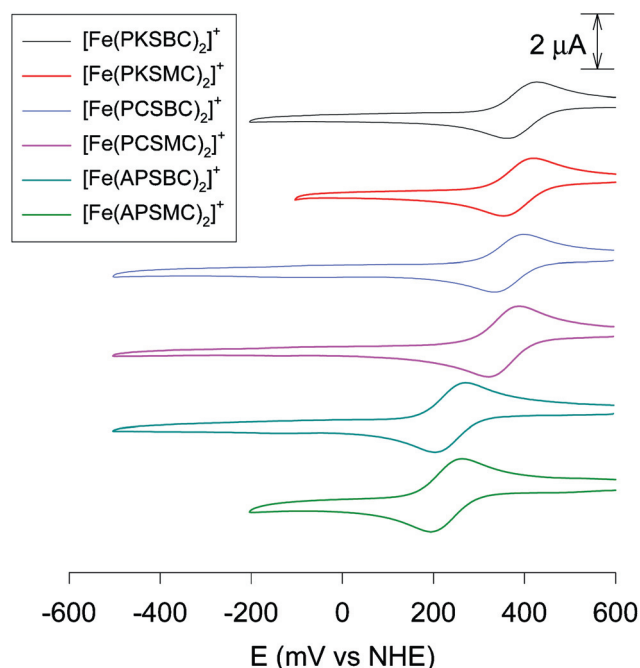


Fig. 6 Cyclic voltammetry of the Fe dithiocarbazate complexes in this work: sweep rate 100 mV s⁻¹, MeCN–H₂O 7:3 solvent and 0.1 M Et₄NClO₄ supporting electrolyte.

complex must be able to be reduced by intracellular reductants (eqn (2)) so the rate of both eqn (1) and (2) will be important in determining the overall yield of $\cdot\text{OH}$. The higher potential Fe^{II} complexes will be less reactive toward H₂O₂ but more easily reduced from their reactive Fe^{III} form.

Cyclic voltammetry of the Fe complexes of the dithiocarbazate ligands was undertaken and the results are summarised in Fig. 6 and Table 3. In all cases the Fe^{II} and Fe^{III} dithiocarbazate complexes gave identical and totally reversible cyclic voltammograms confirming their common structural features (identical first coordination spheres). Only the voltammograms of the Fe^{III} complexes are shown in Fig. 6. Any differences in redox potentials are attributed to changes in inductive effects of the substituents. It is immediately apparent that altering the terminal S-substituent (from methyl to benzyl) has little effect (*ca.*

Table 3 Fe^{III/II} redox potentials and biological data for the chelators in this work

	$E^\circ(\text{Fe}^{\text{III/II}})$ (mV vs. NHE)	IC ₅₀ (μM)	⁵⁹ Fe efflux (% total cell iron released)	⁵⁹ Fe uptake (% control)
Control	—	—	4 ± 0.5	100 ± 4
DFO	–475 (ref. 56)	11.4 ± 0.8	10 ± 2	86 ± 7
H ₂ NIH (311)	—	0.75 ± 0.26	40 ± 3	7 ± 1
HDp44mT	+166 (ref. 28)	0.009 ± 0.004	40 ± 2	4.9 ± 0.8
HAPSMC	+229	0.05 ± 0.02	32 ± 1	18 ± 1
HAPSBC	+239	0.05 ± 0.02	22.4 ± 0.7	46 ± 7
HPKSMC	+383	0.37 ± 0.11	36 ± 2	21 ± 1
HPKSBC	+401	0.09 ± 0.06	28 ± 1	43 ± 11
HPCSMC	+357	>10	38.4 ± 0.9	17 ± 2
HPCSBC	+367	>10	27 ± 3	42 ± 7

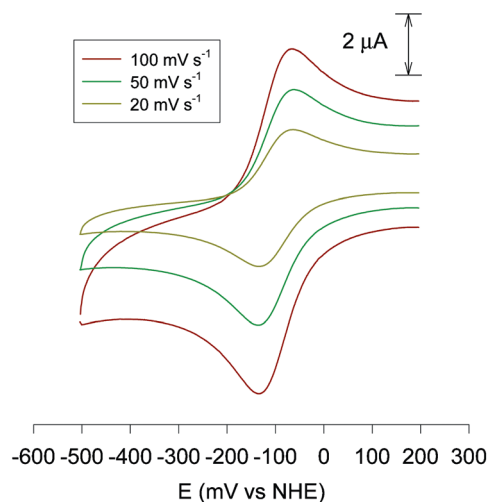


Fig. 7 Cyclic voltammetry of $[\text{Fe}(\text{PSMC})(\text{PCSMC})]$ at 20, 50 and 100 mV s^{-1} sweep rate: MeCN– H_2O (7 : 3) with 0.1 M Et_4NClO_4 supporting electrolyte.

10 mV) on the $\text{Fe}^{\text{III/II}}$ redox potential. This is to be expected given the fact that substitution of a phenyl ring with a H-atom occurs at a position remote from the metal. The substituent on atom C6 (as defined in Fig. 1) has a stronger influence on the redox potential, as found in our investigations of the **HPCIH**¹⁷ and **HDp44mT**³⁰ families and their Fe complexes. The electron-withdrawing non-coordinating pyridyl ring (in **PKSMC**[−] and **PKSBC**[−]) yields Fe complexes with the highest redox potentials of the series. The electron-donating methyl group gave lower potential Fe complexes of **APSMC**[−] and **APSBC**[−]. These potentials were born out in the properties of the Fe^{III} and Fe^{II} complexes; $[\text{Fe}^{\text{II}}(\text{APSMC})_2]$ and $[\text{Fe}(\text{APSBC})_2]$ being air-sensitive in solution upon standing.

The thiosemicarbazone complex $[\text{Fe}(\text{Dp44mT})_2]^+$ (see Chart 1 for ligand structure) exhibits a redox potential (+166 mV)²⁸ more than 200 mV below the analogous thiocarbamate complexes $[\text{Fe}(\text{PKSMC})_2]^+$ and $[\text{Fe}(\text{PKSBC})_2]^+$; all three compounds being of Schiff bases derived from di-2-pyridyl ketone. The thiohydrazone analogue $[\text{Fe}(\text{PKTBH})_2]^+$ (see Chart 1) has a $\text{Fe}^{\text{III/II}}$ redox potential of +383 mV vs. NHE²⁷ which is essentially the same

as that of the thiocarbamate complex analogues reported here. Replacing the thiohydrazone *S*-donor (e.g. $[\text{Fe}(\text{PKTBH})_2]^+$) with an *O*-donor ($[\text{Fe}(\text{PKBH})_2]^+$, a hydrazone) shifts the $\text{Fe}^{\text{III/II}}$ couple to a very high potential (ca. +500 mV) and in fact the highly oxidising Fe^{III} complexes of these and related hydrazone ligands are not stable in aqueous solution.^{16–18}

The redox potential of the unusual mixed-ligand complex $[\text{Fe}(\text{PSMC})(\text{PCSMC})]$ was much lower than the symmetric bis-dithiocarbamate complexes. The voltammetry at three different sweep rates is shown in Fig. 7. Again a totally reversible $\text{Fe}^{\text{III/II}}$ couple is seen, but this time at a potential of −100 mV vs. NHE; approximately 450 mV lower than the related $[\text{Fe}(\text{PCSMC})_2]^+$ complex. This large stabilisation of the trivalent oxidation state is a consequence of the PSMC^{2-} ligand which bears two formally anionic donor atoms; the deprotonated amide N2a (Fig. 5) and the thiolate *S*-donor. This cathodic shift mirrors the behaviour seen in the related hydrazone (**HPCIH**)¹⁶ to hydrazone (**H₂IPH**) series,⁵⁷ where the $\text{Fe}^{\text{III/II}}$ redox potential of $[\text{Fe}^{\text{III}}(\text{IPH})_2]^−$ is ca. 750 mV lower than $[\text{Fe}^{\text{II}}(\text{PCIH})_2]$. In the case of $[\text{Fe}^{\text{III}}(\text{PSMC})(\text{PCSMC})]$, only one of the dithiocarbamate Schiff base ligands has been altered, so the effect on the redox potential is not as pronounced.

Fe mobilisation studies and cytotoxicity

The ability of the dithiocarbamates in Chart 2 to bind intracellular ⁵⁹Fe was examined in two separate, but complementary assays using ⁵⁹Fe₂-Tf which donates ⁵⁹Fe to cells.^{46,47} The ability of the chelators to mobilise cellular ⁵⁹Fe (Fig. 8A) from human SK-N-MC neuroepithelioma cells pre-labelled with ⁵⁹Fe₂-Tf was expressed as the percentage of ⁵⁹Fe released in the presence of each ligand. During this assay, the chelators act as “shuttles” to mobilise ⁵⁹Fe out of the cell. As expected, the control (medium alone with no chelator) resulted in only a small amount (~4%) of ⁵⁹Fe being released from the cell over the time course of the experiment. Positive controls were the known Fe chelators, DFO, **HDp44mT** and **H₂NIH** (311; Chart 1).^{19,46,47} All dithiocarbamate ligands were more effective than DFO at releasing intracellular Fe and **HPCSMC** was the most active of all compounds being almost as effective as **HDp44mT** (Fig. 8A). Furthermore, the three *S*-methyl dithiocarbamates (**HAPSMC**, **HPCSMC** and

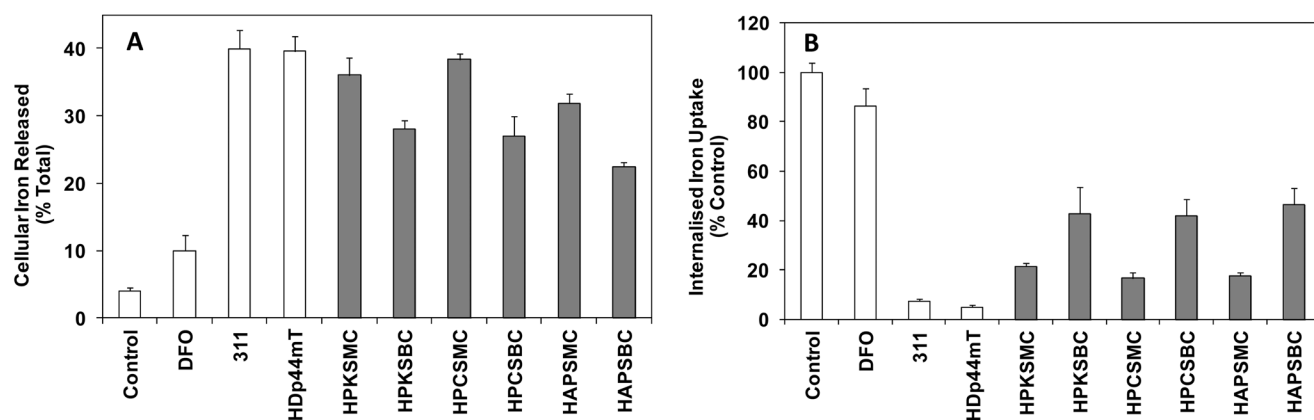


Fig. 8 The effect of the dithiocarbamate chelators on (A) cellular ⁵⁹Fe release from pre-labelled SK-N-MC neuroepithelioma cells and (B) ⁵⁹Fe uptake from ⁵⁹Fe₂-Tf by SK-N-MC neuroepithelioma cells. The control is treated with medium only. Results are mean ± SD (3 experiments). See Charts 1 and 2 for ligand abbreviations.

HPKSMC) were more effective at mobilising intracellular ^{59}Fe than their corresponding *S*-benzyl analogues (HAPSBC, HPCSBC and HPKSBC, respectively).

During the second assay (Fig. 8B), the ability of the chelators to inhibit ^{59}Fe uptake from $^{59}\text{Fe}_2\text{-Tf}$ was assessed. All results are relative to the untreated control (*i.e.* ^{59}Fe in the presence of incubation medium alone). The results mirror those obtained with the ^{59}Fe efflux assay. The three *S*-methyl dithiocarbazates are consistently more effective at preventing ^{59}Fe uptake from $^{59}\text{Fe}_2\text{-Tf}$ than the three *S*-benzyl chelators. Again, the novel chelators prepared in this investigation were all more active than DFO, but less effective than H_2NIH (311) or HDp44mT (Fig. 8B).

Potential chelators for the treatment of Fe overload disorders^{1,2} must have low toxicity as the condition will in many cases require life-long administration of the drug.^{1,2} Thus, the toxicity of the chelators was examined against the same SK-N-MC neuroepithelioma cell line using DFO as a negative control and the highly potent ligand, HDp44mT , as a positive control.^{19,29,46} The results are summarised in Table 3, where it can be seen that the two dithiocarbazates derived from 2-pyridinecarbaldehyde exhibit no apparent cytotoxicity ($>10\ \mu\text{M}$). This property, in combination with their high activity in sequestering intracellular Fe, present ideal properties for a chelator in the treatment of Fe overload. The four dithiocarbazates derived from 2-acetylpyridine and di-2-pyridyl ketone show moderate to potent anti-proliferative activity, and as such, may be problematic as useful drugs for the treatment of Fe overload. However, anti-proliferative activity can be advantageous in the treatment of cancer if a large therapeutic index (anti-proliferative activity against cancer cells relative to normal cells) can be defined, and the thiosemicarbazone relatives are an example of this.^{21,22} This aspect is the subject of a separate investigation.

Conclusions

This study has focused on the Fe coordination chemistry of a series of dithiocarbazate Schiff base ligands. Both Fe^{III} and Fe^{II} complexes were isolated and characterised. Cyclic voltammetry showed that all undergo totally reversible redox reactions at potentials dependent on substituent effects inherent to their parent carbonyl compound (2-acetylpyridine, di-2-pyridyl ketone or 2-pyridinecarbaldehyde). All ligands were more effective in chelating intracellular Fe relative to the clinically proven chelator DFO, and the compounds derived from 2-pyridinecarbaldehyde exhibited no marked anti-proliferative activity. The results reported here mirror the trends observed with the HPCIH, HPKIH and HAPIH hydrazones.¹⁷ In those cases, Schiff bases derived from aldehydes (bearing a H-atom at C6) exhibited no pronounced cytotoxicity in contrast to ketone-derived Schiff bases bearing a methyl, phenyl or pyridyl group at C6 which all exhibited significant anti-proliferative efficacy against cancer cells. Exactly the same trend is seen here, suggesting that the 2-pyridinecarbaldehyde group is an ideal pharmacophore for an Fe chelator with low toxicity as seen in the HPCIH analogues.¹⁶

Acknowledgements

P.V.B. acknowledges financial support from the Australian Research Council (DP1096029). D.R.R. thanks the National

Health and Medical Research Council of Australia for a Senior Principal Research Fellowship and Project Grants. D.S.K. acknowledges the Cancer Institute New South Wales for Early Career Development Fellowship and a Research Innovation Grant. M.T.B. is grateful for scholarship support from the King Abdul Aziz University (Jeddah, Saudi Arabia).

References

- 1 P. V. Bernhardt, *Dalton Trans.*, 2007, 3214–3220.
- 2 P. C. Sharpe, D. R. Richardson, D. S. Kalinowski and P. V. Bernhardt, *Curr. Top. Med. Chem.*, 2011, **11**, 591–607.
- 3 D. M. Frazer, S. J. Wilkins, E. M. Becker, C. D. Vulpe, A. T. McKie, D. Trinder and G. J. Anderson, *Gastroenterology*, 2002, **123**, 835–844.
- 4 D. S. Kalinowski and D. R. Richardson, *Pharmacol. Rev.*, 2005, **57**, 547–583.
- 5 S. Steinhäuser, U. Heinz, M. Bartholomae, T. Weyhermueller, H. Nick and K. Hegetschweiler, *Eur. J. Inorg. Chem.*, 2004, 4177–4192.
- 6 R. Galanello, *Ann. N. Y. Acad. Sci.*, 2005, **1054**, 183–195.
- 7 A. Piga, R. Galanello, G. L. Forni, M. D. Cappellini, R. Origa, A. Zappu, G. Donato, E. Bordone, A. Lavagetto, L. Zanaboni, R. Sechaud, N. Hewson, J. M. Ford, H. Opitz and D. Alberti, *Haematologica*, 2006, **91**, 873–880.
- 8 J. B. Porter, *Drugs Today*, 2006, **42**, 623–637.
- 9 G. J. Kontoghiorghes, M. A. Aldouri, L. N. Sheppard and A. V. Hoffbrand, *Lancet*, 1987, **329**, 1294–1295.
- 10 N. F. Olivieri, G. M. Brittenham, C. E. McLaren, D. M. Templeton, R. G. Cameron, R. A. McClelland, A. D. Burt and K. A. Fleming, *N. Engl. J. Med.*, 1998, **339**, 417–423.
- 11 J. Savulescu, *Br. Med. J.*, 2004, **328**, 358–359.
- 12 F. H. Mourad, A. V. Hoffbrand, M. Sheikh-Taha, S. Koussa, A. I. Khoriaty and A. Taher, *Br. J. Haematol.*, 2003, **121**, 187–189.
- 13 E. Becker and D. R. Richardson, *J. Lab. Clin. Med.*, 1999, **134**, 510–521.
- 14 C. S. M. Wong, J. C. Kwok and D. R. Richardson, *Biochim. Biophys. Acta, Mol. Basis Dis.*, 2004, **1739**, 70–80.
- 15 D. B. Lovejoy, D. S. Kalinowski, P. V. Bernhardt and D. R. Richardson, *Hemoglobin*, 2006, **30**, 93–104.
- 16 P. V. Bernhardt, P. Chin, P. C. Sharpe and D. R. Richardson, *Dalton Trans.*, 2007, 3232–3244.
- 17 P. V. Bernhardt, G. J. Wilson, P. C. Sharpe, D. S. Kalinowski and D. R. Richardson, *J. Biol. Inorg. Chem.*, 2008, **13**, 107–119.
- 18 P. V. Bernhardt, L. M. Caldwell, T. B. Chaston, P. Chin and D. R. Richardson, *J. Biol. Inorg. Chem.*, 2003, **8**, 866–880.
- 19 J. Yuan, D. B. Lovejoy and D. R. Richardson, *Blood*, 2004, **104**, 1450–1458.
- 20 M. Whitnall, J. Howard, P. Ponka and D. R. Richardson, *Proc. Natl. Acad. Sci. U. S. A.*, 2006, **103**, 14901–14906.
- 21 Y. Yu, D. S. Kalinowski, Z. Kovacevic, A. R. Sifakas, P. J. Jansson, C. Stefani, D. B. Lovejoy, P. C. Sharpe, P. V. Bernhardt and D. R. Richardson, *J. Med. Chem.*, 2009, **52**, 5271–5294.
- 22 Z. Kovacevic, D. S. Kalinowski, D. B. Lovejoy, Y. Yu, Y. S. Rahmanto, P. C. Sharpe, P. V. Bernhardt and D. R. Richardson, *Curr. Top. Med. Chem.*, 2011, **11**, 483–499.
- 23 J. G. Cory, A. H. Cory, G. Rappa, A. Lorico, M.-C. Liu, T.-S. Lin and A. C. Sartorelli, *Biochem. Pharmacol.*, 1994, **48**, 335–344.
- 24 M.-C. Liu, T.-S. Lin, P. Penketh and A. C. Sartorelli, *J. Med. Chem.*, 1995, **38**, 4234–4243.
- 25 M.-C. Liu, T.-S. Lin and A. C. Sartorelli, *Prog. Med. Chem.*, 1995, **32**, 1–35.
- 26 R. A. Finch, M. Liu, S. P. Grill, W. C. Rose, R. Loomis, K. M. Vasquez, Y. Cheng and A. C. Sartorelli, *Biochem. Pharmacol.*, 2000, **59**, 983–991.
- 27 D. S. Kalinowski, P. C. Sharpe, P. V. Bernhardt and D. R. Richardson, *J. Med. Chem.*, 2007, **50**, 6212–6225.
- 28 D. R. Richardson, P. C. Sharpe, D. B. Lovejoy, D. Senaratne, D. S. Kalinowski, M. Islam and P. V. Bernhardt, *J. Med. Chem.*, 2006, **49**, 6510–6521.
- 29 D. S. Kalinowski, Y. Yu, P. C. Sharpe, M. Islam, Y.-T. Liao, D. B. Lovejoy, N. Kumar, P. V. Bernhardt and D. R. Richardson, *J. Med. Chem.*, 2007, **50**, 3716–3729.
- 30 D. R. Richardson, D. S. Kalinowski, V. Richardson, P. C. Sharpe, D. B. Lovejoy, M. Islam and P. V. Bernhardt, *J. Med. Chem.*, 2009, **52**, 1459–1470.

- 31 M. Akbar Ali, A. H. Mirza, M. Nazimuddin, H. Rahman and R. J. Butcher, *Polyhedron*, 2001, **20**, 2431–2437.
- 32 M. R. Maurya, S. Khurana, W. Zhang and D. Rehder, *Eur. J. Inorg. Chem.*, 2002, 1749–1760.
- 33 M. Akbar Ali, A. H. Mirza, M. Nazimuddin, R. Ahmed, L. R. Gahan and P. V. Bernhardt, *Polyhedron*, 2003, **22**, 1471–1479.
- 34 A. M. Akbar, A. H. Mirza, T. B. S. A. Ravooof and P. V. Bernhardt, *Polyhedron*, 2004, **23**, 2031–2036.
- 35 A. M. Akbar, A. H. Mirza, F. H. Bujang, M. H. S. A. Hamid and P. V. Bernhardt, *Polyhedron*, 2006, **25**, 3245–3252.
- 36 A. B. Beshir, S. K. Guchhait, J. A. Gascon and G. Fenteany, *Bioorg. Med. Chem. Lett.*, 2008, **18**, 498–504.
- 37 T. B. S. A. Ravooof, K. A. Crouse, M. I. M. Tahir, F. N. F. How, R. Rosli and D. J. Watkins, *Transition Met. Chem.*, 2010, **35**, 871–876.
- 38 S. Shrivastava, N. Fahmi, D. Singh and R. V. Singh, *J. Coord. Chem.*, 2010, **63**, 1807–1819.
- 39 A. M. Akbar, A. H. Mirza, R. J. Butcher, P. V. Bernhardt and M. R. Karim, *Polyhedron*, 2010, **30**, 1478–1486.
- 40 B. K. Koo, *Bull. Korean Chem. Soc.*, 2011, **32**, 1729–1732.
- 41 A. Molter, J. Rust, C. W. Lehmann, G. Deepa, P. Chiba and F. Mohr, *Dalton Trans.*, 2011, **40**, 9810–9820.
- 42 M. Akbar Ali, S. E. Livingstone and D. J. Phillips, *Inorg. Chim. Acta*, 1971, **5**, 493–498.
- 43 R. Raina and T. S. Srivastava, *Inorg. Chim. Acta*, 1984, **91**, 137–140.
- 44 W.-X. Hu, W. Zhou, C.-N. Xia and X. Wen, *Bioorg. Med. Chem. Lett.*, 2006, **16**, 2213–2218.
- 45 P. Bera, C.-H. Kim and S. I. Seok, *Polyhedron*, 2008, **27**, 3433–3438.
- 46 D. R. Richardson, E. H. Tran and P. Ponka, *Blood*, 1995, **86**, 4295–4306.
- 47 D. R. Richardson and E. Baker, *Biochim. Biophys. Acta, Mol. Cell Res.*, 1990, **1053**, 1–12.
- 48 D. R. Richardson and K. Milnes, *Blood*, 1997, **89**, 3025–3038.
- 49 G. M. Sheldrick, *Acta Crystallogr., Sect. A*, 2008, **64**, 112–122.
- 50 L. J. Farrugia, *J. Appl. Crystallogr.*, 1997, **30**, 565.
- 51 L. J. Farrugia, *J. Appl. Crystallogr.*, 1999, **32**, 837–838.
- 52 A. L. Spek, *Acta Crystallogr., Sect. D*, 1990, **65**, 148–155.
- 53 J. P. Scovill and J. V. Silverton, *J. Org. Chem.*, 1980, **45**, 4372–4376.
- 54 D. Richardson, P. V. Bernhardt and E. M. Becker, *2-Pyridinecarboxaldehyde Isonicotinoylhydrazone Iron Chelators and Uses thereof*, University of Queensland, Heart Research Institute Ltd., Australia, WO, 2001.
- 55 H. B. Dunford, *Coord. Chem. Rev.*, 2002, **233–234**, 311–318.
- 56 I. Spasojevic, S. K. Armstrong, T. J. Brickman and A. L. Crumbliss, *Inorg. Chem.*, 1999, **38**, 449–454.
- 57 P. V. Bernhardt, P. Chin, P. C. Sharpe, J.-Y. C. Wang and D. R. Richardson, *J. Biol. Inorg. Chem.*, 2005, **10**, 761–777.